Master's Thesis

Multi-sector cooperation in multi-user MIMO for a measured urban macro-cellular environment

by

Ningxin Chen

Department of Electrical and Information Technology
LTH, Lund University
SE-221 00 Lund, Sweden

Abstract

This master thesis mainly studies the benefits of multi-sector cooperation in the radio base station (BS) of a multi-user multiple-input multiple-output (MU-MIMO) system. The performance evaluation is performed using intra-site coordinated multi-point (CoMP) channel measurements in an urban macrocellular environment at the carrier frequency of 2.65 GHz. The focus of the analysis is to investigate the MU-MIMO capacity gain enabled by three-sector cooperation in a single BS site for both multiple access channel (MAC) and broadcast channel (BC). To simplify the complexity of the calculation, we study the two-user scenario. To calculate the sum rate capacity, joint decoding is assumed in the MAC case. Due to the complexity in the maximization of the transmit covariance matrix and the minimization of the noise correlation matrix in the BC case, uplink-downlink duality between MAC and BC is applied to obtain the capacity in the BC case. The results show that the median MU-MIMO capacity gain introduced by the three-sector cooperation is about 30% and 80% in MAC and BC, respectively. When it comes to the outage performance, 10% of the measured positions have capacity gains of over 65% and 110%, in MAC and BC, respectively. Furthermore, when one user is fixed at the center of each sector, the capacity gain is maximum when the other user moves to the back lobe of the sector. On the other hand, when one user is fixed at the edge of two neighboring sectors, the capacity can be greatly improved when the other user moves into the coverage area of the third sector. The same conclusions can be obtained in both MAC and BC cases. To summarize, using multi-sector cooperation in an intrasite CoMP system exhibits great potential for improving the capacity performance in MU-MIMO systems.

Acknowledgments

This Master's thesis would not exist without the support and guidance of Dr. Buon Kiong Lau at the Department of Electrical and Information Technology at Lund University. I am very grateful that you share your deep knowledge in the field of wireless communication, especially Multiple Antenna Technology, with me. And through the daily conversation during lunch, you taught me a lot of things, which help me to have a different point of view towards research and life in general. In addition, thank you very much for the advice on how to do a good presentation, which played an important role during the preparation of my thesis presentation.

I would like to offer my heartfelt thanks to Dr. Ruiyuan Tian, who co-supervised the thesis work. Thank you very much for your patience and suggestions during every discussion. Your suggestions and technical support are very important to my master's thesis project. And thank you for being a good friend and helping me face all the pressure in performing the thesis work.

I also thank Dr. Jonas Medbo of Ericsson Research, Kista, Stockholm, for providing the measurement data used in this project.

Finally, I acknowledge the kind support of Pol Henarejos and Prof. Ana I. Perez Neira of Centre Tecnològic de Telecomunicacions de Catalunya (CTTC), Barcelona, Spain, in the MATLAB implementation of the BC sum capacity.

Ningxin Chen
Lund
March, 2012

Table of Contents

CHAPTER 1

1 Introduction

1.1 Background

1.1.1 LTE and LTE Advanced

LTE (Long Term Evolution) is a promising radio communication technology which evolved from the third-generation UMTS (Universal Mobile Telecommunication System) technology [1]. LTE can provide the maximum data rate of 300 Mbps in the downlink and 50 Mbps in the uplink. QPSK, 16QAM and 64QAM modulation schemes are used. The Radio Access Technology is OFDMA in the downlink and SC-FDMA in the uplink. Compared to UMTS, LTE can dramatically increase the spectral efficiency and therefore system capacity. Since LTE will use the same frequency bands as UMTS, a gradual migration of the old system to the new system is planned.

In order to realize even higher data rates of up to 1 Gbps for low mobility user and 100 Mbps for high mobility user, LTE-Advanced (LTE-A) has been studied. As an evolution of LTE, LTE-A can support wider frequency bandwidths through the technique of Carrier Aggregation (CA). CA allows the aggregation of different numbers of carriers from different bands in either downlink or uplink [1]. In addition, Multiple-Input Multiple-Output (MIMO) technology including Single User (SU)-MIMO and Multiuser (MU)-MIMO has been proposed in LTE-A in order to achieve the targets of higher peak data rates, bigger cell coverage and increased cell throughput.

1.1.2 MIMO

Due to the increasing demand for higher data rates, better quality of service (QoS), higher network capacity, increased spectral efficiency and link reliability, MIMO emerges as an enabling technology which can improve the performance of wireless communications in these aspects [2].

The main benefit of MIMO is in the form of spatial multiplexing [3]. The spatial multiplexing scheme allows multiple transmit (TX) antennas to send different bit streams to multiple receive (RX) antennas in order to greatly improve the system throughput.

Using a number of TX and RX antennas, the spatial multiplexing scheme can make efficient use of the spatial resource such that it can offer a linear increase in system capacity. To be more specific, if there are N_T antennas at the transmitter, and N_R antennas at the receiver, the channel capacity can be increase by an order of $N_S = min(N_T, N_R)$.

In addition, MIMO also offers the benefit of diversity gain, which increases the system reliability by mitigating multipath fading. In particular, when multiple TX antennas send the same signal to multiple RX antennas, even though the signals at some RX antennas may suffer from deep fades during the transmission, it is still possible that other RX antennas get sufficient signal quality. In this way, the symbol error rate is greatly reduced.

1.1.3 MU-MIMO

With the growing understanding of the theoretical knowledge of MIMO, and due to the potential of increasing the system reliability and capacity, MIMO can be considered the most important technology in modern wireless communications. However, the early research in MIMO considers only point-to-point communication, which is the case of SU-MIMO. In order to incorporate MIMO into the more practical multi-user context, more and more researchers have begun to focus on the development of MU-MIMO, instead of SU-MIMO. MU-MIMO [4] is a cellular communication system which enables the simultaneous use of more than one terminal (or user) during the communication, while SU-MIMO can only afford one terminal (or user). MU-MIMO will be introduced in the following.

As a key technology in wireless communication, MU-MIMO has the following potential benefits compared to SU-MIMO [4]-[6]:

(1) It suffers less from antenna correlation effect as compared to SU-MIMO. Even though antenna correlation still affects the diversity on the per-user basis, it is not a major issue for the MU-MIMO system diversity;

(2) Spatial multiplexing gain is achieved at the base station (BS) without the need of multiple antennas equipped at the user, which reduces the cost on the terminal side;

(3) The spatial domain can offer an additional degree of freedom, which can be exploited by multiuser diversity;

(4) MU-MIMO system is more robust due to high multipath richness and low correlation between the antennas on the user side.

According to Fig. 1.1, MU-MIMO can be divided into two kinds of channels according to the direction of information transmission. In the downlink case, the M-antenna BS transmits K data streams to the K users (or terminals). This is known as the Broadcast Channel (BC). On the other hand, the uplink is called the Multiple Access Channel (MAC). The algorithms for the capacity calculation of the BC and MAC cases will be explained in detail in Chapter 3.

A large amount of theoretical research has been conducted in the field of MU-MIMO. The performance of MU-MIMO depends on three factors [7]:

(1) Precoding scheme at the transmitter side;

(2) Quality of the channel state information (CSI);

(3) Channel characteristic and user separation.

In [8], it is found that, using the interference rejection combining receiver, the capacity improvement can be maximized for the condition of small angular spread with co-polarized and closely spaced uniform linear arrays at the BS. In order to get accurate CSI, [9] proposed a feedback mechanism of using spatial correlation information from the users' channels to design codebook. In [10], the authors present a system level simulation to obtain different TX correlation performance. In [11], a joint TX-RX user scheduling scheme is proposed to help the BS have better CSI and hence optimize the channel performance.

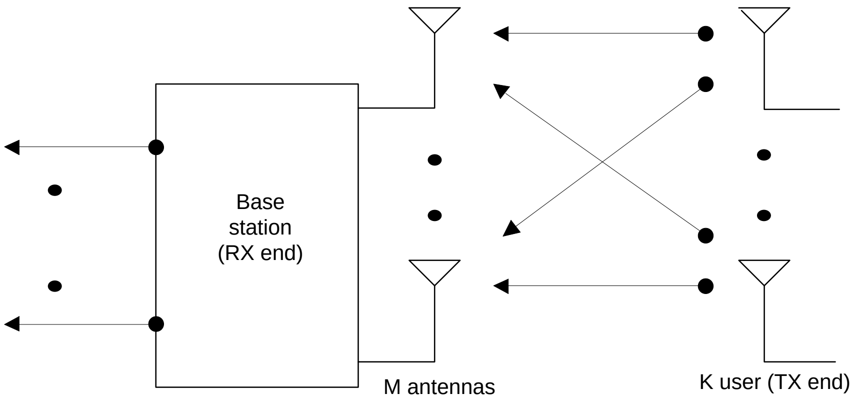

(a) MAC

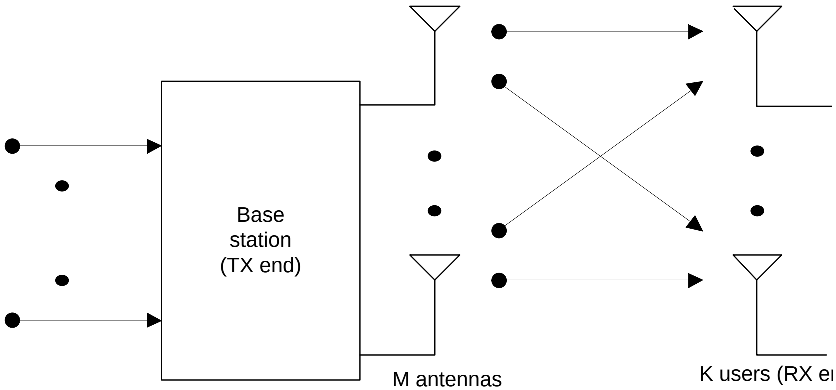

(b) BC

Fig. 1.1 Uplink (MAC) and downlink (BC) scenarios of MU-MIMO.

1.1.4 CoMP

In order to achieve high data rates [12] and increase system coverage, coordinated multi-point (CoMP) transmission/reception is introduced as a promising technology. CoMP is able to exploit or mitigate the interference between different sectors or sites. It can increase the data rate, especially for the users at the cell edge. As an integral part of LTE, CoMP is categorized in two forms [13]: cooperation among multi-sectors in one BS (intrasite coopration) and cooperation among multiple BSs (intersite cooperation). While a lot of work has been done for intersite cooperation, less attention has been given to intrasite cooperation.

Intersite Cooperation

Interference from neighboring BSs is the main factor affecting the spectral efficiency of a cellular system. To solve this problem, cooperation among different BSs (or BS sites) is introduced. Joint processing and coordinated scheduling are two types of intersite cooperation. In joint processing, a number of BSs can transmit a signal together to a user terminal, which can improve the signal-to-interference-and-noise ratio (SINR) at the given terminal. However, this approach may deteriorate the SINR at other terminals. More efficiently, the cooperating BSs can choose a precoding matrix that matches the channel to the terminal and creates little interference to other terminals at the same time [12]. Overall, joint processing will cause latency and higher sensitivity to channel estimation error, which lead to the greater popularity of coordinated scheduling.

Furthermore, the work performed in [14] shows that, by increasing the rank of the channel instead of decreasing the interference, cooperation offers new spatial degrees of freedom, which in turn increases the spectral efficiency compared to the conventional frequency reuse system. Alternatively, by using limited (i.e., localized) base station cooperation [15] with highly directive antennas, spectral efficiency is increased especially in metropolitan and urban macrocellular scenarios. Co-channel interference is reduced by employing multiuser eigenmode transmission and MMSE. In [16], through adjusting the tilt angle of the base station antennas, inter-cell interference is mitigated directly.

Intrasite Cooperation

As opposed to intersite cooperation, intrasite cooperation involves different sectors of the same BS site. This leads to a simpler implementation of coordinated processing and therefore a better tradeoff between complexity and performance improvement [3].

For intrasite cooperation, the problem of limited angular spread in the signal can be alleviated. The terminal of interest can receive the signal from the back lobe(s) of neighboring sector(s) and/or reflection from the main lobe(s) of neighboring sector(s), which increase the angular spread compared to when there is only one serving sector, which is beneficial for multi-stream MIMO operation.

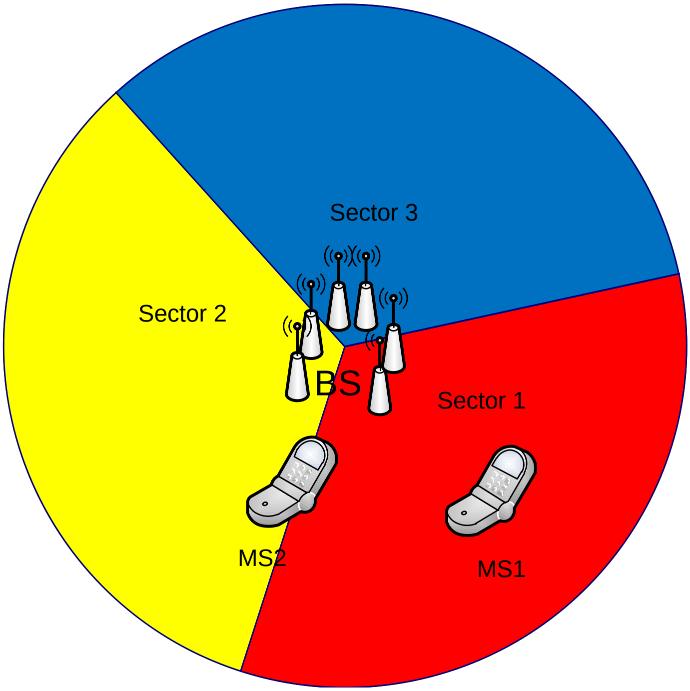

Fig. 1.2. Multi-user sector cooperation

Figure 1.2 describes a scenario of a BS (consisting of a three-sector antenna system) communicates with two terminals at the same time in an urban macro-cellular environment. Without sector cooperation, there is only one sector serving the two terminals at any given time[1]. According to the directional nature of the antenna, each sector has its main lobe direction and coverage area. If one terminal is located at the edge non-serving sectors, this user can only receive the signal via reflection(s) of the signal at the serving sector (if signal from the back lobe is negligible). In this condition, the user will have low power gain, which severely decreases the performance of the overall communication system. However, through sector cooperation, each user can received signals from the (fixed) serving sector as well as the neighboring sectors, which can greatly improve the sum capacity performance of the overall system. Besides, intrasite cooperation increases the number of antennas used for communication, which will also improve the system capacity.

[1] It should be noted that, in general, the reference case (without cooperation) should allow *each* of the two users to be served by the sector with the strongest link. In this thesis, we only study the simpler reference case with only one sector serving the two users.

1.2 Previous work

Apart from the literature review already provided in the previous sections, a Master's thesis project on multi-sector cooperation with SU-MIMO in a measured urban environment has been performed[2]. The results from the project show that the capacity gain through cooperation can exceed 40% in 25% of the coverage area. Moreover, the greatest increase occurs near the edge of two neighboring sectors.

Among existing papers on intrasite cooperation, [13] proposed that intrasite cooperation is easier to realize than intersite cooperation in the real world from the economic point of view, which indicates that the research in this field can contribute more to the implementation of real systems. Moreover, intrasite cooperation has been considered to have obvious advantages over intersite cooperation, including direct synchronization, no limitations in the amount data exchange or delay [6]. In fact, the uplink part has already been realized in real systems: Joint detection and power control are taken into consideration in enhancing the system performance.

1.3 Objectives

The objective of this thesis is to quantify the performance improvement in MU-MIMO systems through sector cooperation in a real world urban macrocellular environment. The system performance is mainly measured in the form of multi-user sum rate capacity. Comparisons are made for both MAC and BC.

1.4 Organization

The rest of the thesis is organized as follows. Chapter 2 describes how the measurement was set up. The algorithms for calculating the sum rate capacity for the uplink and downlink cases are provided in Chapter 3. Uplink (MAC) results and analysis are presented at Chapter 4. Downlink

---

[2] B. Wu, "Polarization and multi-sector cooperative MIMO in a measured urban macrocellular environment," *MSc Thesis*, Department of Electrical and Information Technology, Lund University, Sweden, Jun. 2011.

(BC) results and analysis are given in Chapter 5. Finally, conclusions are drawn in Chapter 6 and some future works are suggested in Chapter 7.

1.5 Contributions

In this Master's thesis, through the calculation of sum rate capacity in both the MIMO-MAC and MIMO-BC cases, the effectiveness of sector cooperation in improving system capacity is shown. Apart from the actual results, the thesis also provides the framework for the analysis of such systems in a real world context.

CHAPTER 2

2 Measurement Setup

The measurement was carried out in the urban area of Kista (also called “Mobile Valley”), Stockholm, Sweden. The BS coverage area was divided into three $120°$ sectors. Each sector was equipped with a $\pm 45°$ cross-polarized directional antenna pair mounted a few meters above the rooftop of the building. The rooftop was about 34 m above the street level. The terminal (or mobile station) was a measurement van equipped with two vertical and two horizontal dipole antennas on its roof. The four antennas were placed at the four corners of a square configuration, which had the side spacing of approximately 30 cm (i.e., 2.6 wavelengths at the center frequency of 2.65 GHz). A snapshot of the 20 MHz channel was recorded every 5.33 ms. The channel transfer functions between all pairs of TX and RX antennas were measured coherently by an Ericsson channel sounder.

The drive route of the terminal is shown using the blue line in Fig. 2.1, where the start position of the route is shown by the number “1” in the lower left part of the figure. The drive route goes around the BS (indicated by a green triangle) in a clockwise direction. A total of 67001 locations were measured along the entire route. For each of the 67001 locations, 162 frequency samples (over 20 MHz) of the 4×6 MIMO channel were recorded. All relevant parameters in the measurement are described in Table 2.1. Besides, to simplify the calculation of sum rate capacity in the downlink, we only choose one vertical and one horizontal dipole antenna at the terminal end, resulting in the channel matrix of dimensions 2×6 ($\times$ 162 frequency bins).

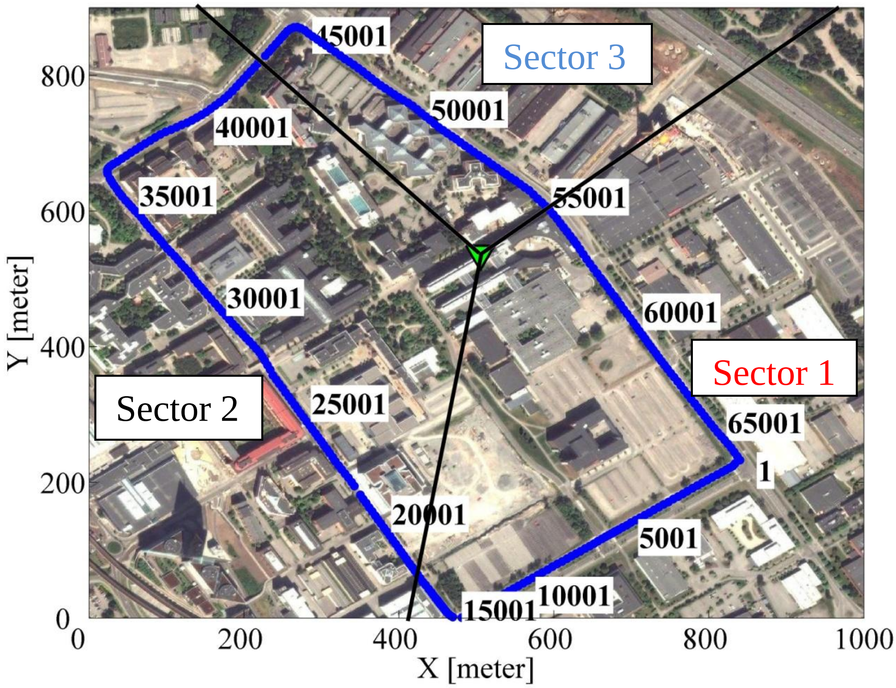

Fig. 2.1 Drive route with sector distribution

TABLE 2.1 SPECIFICATIONS OF THE ERICSSON CHANNEL SOUNDER AND ANTENNA SYSTEM SETUP

Parameter	**Value**
Number of BS Sector	3
Number of BS antennas	2
Number of terminals	1
Number of terminal antennas	4
Center Frequency	2.65 GHz
Bandwidth	20 MHz
Number of frequency bins	162
Number of measured locations	67001
Measurement time interval	5.33 ms

Because it is the multiuser case, the number of users should be equal to or larger than 2. To study this case, we can assume that each measurement location along the drive route can represent an individual user (if the channel is stationary). However, in order to reduce the complexity of calculation and to gain fundamental insights into multiuser operation, we choose to consider only two users in this thesis.

Fig. 2.2 Coverage area of Sector 1.

Fig. 2.3 Coverage area of Sector 2.

Fig. 2.4 Coverage area of Sector 3.

In addition, if the two users are allow to be located at two arbitrary measurement locations of the drive route together, there can be up to 67001×67001 samples for the capacity calculation. In order to simplify the math, we set one user to be located in one fixed position, whereas the other user moves along the entire route. The position of the fixed user can then be changed in order to analyze a different user scenario.

To better understand the propagation condition of each sector in the BS site, Figs. 2.2 to 2.4 show the coverage areas of the three sectors, respectively. The center of each photo roughly corresponds to the direction of maximum gain of the sector antenna.

For Sector 1, it is obvious from Fig. 2.2 that there is almost no obstacle that blocks the line-of-sight (LOS) path between the BS and the terminal, except for one red building. The height of the antenna in Sector 1 is higher than most of the other objects. Therefore, we can conclude that this scenario is mostly LOS. However, the conditions for Sectors 2 and 3 are different from that of Sector 1 (see Figs. 2.3 and 2.4). Due to the dense office buildings, the propagation scenario is non-LOS (NLOS) in a majority of the measurement locations here. In addition, there is a skyscraper in Fig. 2.3, which can cause a large decrease in signal reception in that direction.

CHAPTER 3

3 MU-MIMO Capacity

3.1 MIMO-MAC

3.1.1 Signal Model

Consider a system with M antennas at the BS and K users, with each user (terminal) equipped with one antenna. This model can be generalized to multiple antennas at each user, as will be done in the following. It is assumed that the channel is frequency flat, with the total average power constraint $\sum_{k=1}^{K} p_k = P$ and the TX side having the full knowledge of the CSI [4].

The uplink channel is given as:

$$\boldsymbol{y} = \mathbf{H}\boldsymbol{s} + \boldsymbol{n}\ , \qquad (3\text{-}1)$$

where $\boldsymbol{y}$ is a $M \times 1$ vector, $\mathbf{H} = [\boldsymbol{h}_1 \boldsymbol{h}_2 \dots \boldsymbol{h}_K]$ is a $M \times K$ forward link channel matrix, $\boldsymbol{s} = [s_1 s_2 \dots s_K]^T$ is a $K \times 1$ vector and $\boldsymbol{n} = [n_1 n_2 \dots n_M]^T$ is the $M \times 1$ addictive complex Gaussian noise vector.

In our case, if there is only one serving sector, then $M = 2$ antennas at the BS. We also have $K = 2$ users, while each user is equipped with two antennas. The uplink channel $\boldsymbol{y}$ is then a 2×1 vector, and $\mathbf{H} = [\mathbf{H}_1 \mathbf{H}_2]$ is a 2×4 channel matrix, while both $\mathbf{H}_1$ and $\mathbf{H}_2$ are 2×2 matrices, $\boldsymbol{s} = [\boldsymbol{s}_1 \boldsymbol{s}_2]^T$ is a 4×1 vector and $\boldsymbol{n} = [n_1 n_2]^T$ is the 2×1 addictive Gaussian noise vector.

If there exists three sectors cooperation, then $M = 6$ antennas at the BS and we also have $K = 2$ users, each with two antennas. Considering that the uplink channel $\boldsymbol{y}$ is a 6×1 vector, $\mathbf{H} = [\mathbf{H}_1 \mathbf{H}_2]$ is a 6×4 channel matrix, while both $\mathbf{H}_1$ and $\mathbf{H}_2$ are 6×2 matrices, $\boldsymbol{s} = [\boldsymbol{s}_1 \boldsymbol{s}_2]^T$ is a 4×1 vector and $\boldsymbol{n} = [n_1 n_2 \dots n_6]^T$ is the 6×1 addictive complex Gaussian noise vector.

3.1.2 Joint decoding

A prime pursuit of current wireless communication is to get higher symbol rates in the system. To fulfill the target, many technologies, such as Code Division Multiple Access (CDMA) and MIMO, are applied to increase the channel capacity for a given amount of spectrum. Channel capacity [17] stands for the rate at which we can transfer signals reliably under a certain signal-to-noise ratio (SNR). For the multi-user operation, another important factor in determining the achievable sum capacity rate is the decoding scheme used. In the MAC case, we consider joint decoding, which implies that the signals are decoded in a cooperative manner.

According to [17], the capacity region should satisfy:

$$\sum_{p\in\Gamma} R_p \le \log_2 \det(\mathbf{I}_M + \frac{1}{N_0}\mathbf{H}_\Gamma \mathbf{R}_{SS,\Gamma}\mathbf{H}_\Gamma^H) \ , \qquad (3\text{-}2)$$

Where p represents a subset of the set $\Gamma = \{1, 2, \dots, K\}$, $\mathbf{H}_p$ and $\mathbf{R}_{SS,p}$ are the channel and transmit covariance matrices corresponding to the subset *p*, respectively.

For a two-user system, the capacity region is:

$$R_1 \le \log_2(1 + \frac{E_{s,1}}{N_0}\|\mathbf{H}_1\|_F^2) \ , \qquad (3\text{-}3)$$

$$R_2 \le \log_2(1 + \frac{E_{s,2}}{N_0}\|\mathbf{H}_2\|_F^2) \ , \qquad (3\text{-}4)$$

$$R_1 + R_2 \le \log_2 det(I_2 + \frac{E_{s,1}}{N_0}\mathbf{H}_1\mathbf{H}_1^H + \frac{E_{s,2}}{N_0}\mathbf{H}_2\mathbf{H}_2^H) \ . \qquad (3\text{-}5)$$

The rate region is shown in the following Fig. 3.1. R_1 is the maximum capacity for user 1 while considering user 2 as interference, while R_2 is the opposite case. According to the formula in (3-3), we find that R_1 mainly depends on the SNR and channel strength of $\mathbf{H}_1$, and so does R_2. Line AB is the sum rate $R_1 + R_2$, which is maximum achievable capacity obtained by each user transmitting at the maximum power. When $\mathbf{H}_1$ is orthogonal to $\mathbf{H}_2$, there is no interference to each other, so the result is the maximum sum rate capacity. However, if $\mathbf{H}_1$ is parallel to $\mathbf{H}_2$, the two users can hardly be separated, so one will get the minimum sum rate capacity.

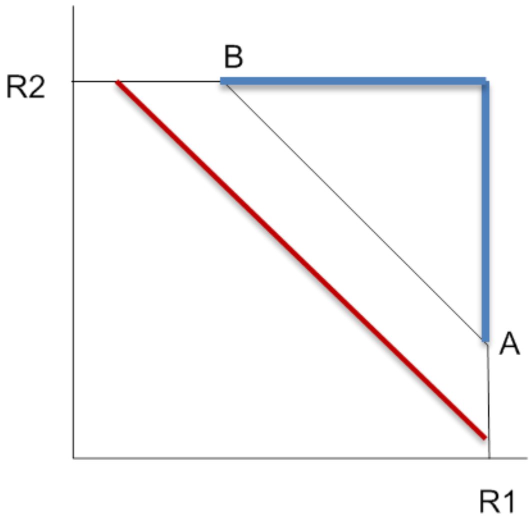

Fig. 3.1 Capacity region for two user MAC channel.

3.2 MIMO-BC

3.2.1 Signal Model

Assume a flat frequency channel, with the total average power constraint given by $\sum_{k=1}^{K} p_k = P$, and the BS has the perfect knowledge of the CSI. Signals are transmitted through a different vector channel to each of the K users.

The downlink model is given as:

$$\boldsymbol{y} = \mathbf{H}\boldsymbol{s} + \boldsymbol{n}$$

where $\boldsymbol{y} = [y_1 y_2 \dots y_K]^T$ is a $K \times 1$ vector, $\mathbf{H}$ is a $K \times M$ forward link channel matrix, $\boldsymbol{s} = [s_1 s_2 \dots s_M]^T$ is a $M \times 1$ vector and $\boldsymbol{n} = [n_1 n_2 \dots n_K]^T$ is the $K \times 1$ addictive complex Gaussian noise vector.

In our case, if there is only one serving sector in BS, $M = 2$ antennas at the BS. We have $K = 2$ users and each user is equipped with two antennas.

The downlink channel $\boldsymbol{y}$ is then a 2×1 vector, and $\mathbf{H} = [\mathbf{H}_1 \mathbf{H}_2]^T$ is a 2×2 channel matrix, while both $\mathbf{H}_1$ and $\mathbf{H}_2$ are 2×2 matrices, $\boldsymbol{s} = [s_1 s_2]^T$ is a 2×1 vector and $\boldsymbol{n} = [n_1 n_2]^T$ is the 2×1 addictive complex Gaussian noise vector.

If we consider the cooperation case, $M = 6$ antennas at the BS and we also have $K = 2$ users, each with two antennas. Considering that the uplink channel $\boldsymbol{y}$ is a 4×1 vector, $\mathbf{H} = [\mathbf{H}_1; \mathbf{H}_2]$ is a 4×6 channel matrix, while both $\mathbf{H}_1$ and $\mathbf{H}_2$ are 2×6 matrices, $\boldsymbol{s} = [s_1 s_2 s_3 s_4 s_5 s_6]^T$ is a 6×1 vector and $\boldsymbol{n} = [n_1 n_2 \dots n_4]^T$ is the 4×1 addictive complex Gaussian noise vector.

3.2.2 Dirty Paper Coding

The degraded channel is one where the channel degrades the signals between the source and the first receiver, and degrades the signals more before the second receiver. Therefore, the Gaussian broadcast channel is always considered as non-degraded channel.

However, the sum rate capacity of the Gaussian broadcast channel has been an open problem until now. To calculate the sum rate capacity of MIMO-BC, the dirty paper coding method according to the research of Costa [18] has been introduced. If the transmitter has full knowledge of the interference, the capacity is the same as when there is no interference.

The Gaussian channel with interference can be described as:

$$y = s + i + w \tag{3-6}$$

where $i \sim N(0, Q)$ is the interference, $w \sim N(0, N)$ is the Gaussian noise.

If the signal power constraint is $|s|^2 \le P$, then the sum rate capacity is

$$C = \frac{1}{2} \log\left(1 + \frac{P}{N}\right) \tag{3-7}$$

Furthermore, the calculation of the capacity region for MIMO-BC includes both the maximization of the transmit covariance matrix and minimization of the noise correlation matrix, which is extremely complex to calculate.

3.2.3 Duality

To solve the maximization problem, duality between the Gaussian broadcast channel and the Gaussian vector multiple access channel is introduced [19], [20].

Under the same power constraint, if we exchange the input and output, and transpose the channel matrix, the capacity of the BC and MAC will be the same. The power on the BS side is the same as the sum value on the terminal side, and the singular value of the channel matrix $\mathbf{H}$ and its transpose $\mathbf{H}^T$ are identical. This is true even when the channel matrix is not square.

The following algorithm has been developed by Yu [21]. Using duality, the sum rate capacity can be obtained as:

$$\text{Maximize} \quad \frac{1}{2}\log\frac{\left|\sum_{k=1}^{K}\mathbf{H}_k\mathbf{S}_k\mathbf{H}_k^T+\mathbf{S}_z\right|}{|\mathbf{S}_z|}, \tag{3-8}$$

subject to

$$\sum_{k=1}^{K} tr(\mathbf{S}_k) \leq P,$$

$$\mathbf{S}_k \geq 0,\, k = 1, \dots, K.$$

The algorithm to calculate the sum power constraint of the dual Gaussian multiple access channel is given below:

(a) Initialize $l_{min} = 0$ and $l_{max} = P$.

(b) Set $ll = (l_{min} + l_{max})/2$

(c) Set $\gamma = 0.1$ in practice

(d) Use water filling to find the optimal $(\mathbf{S}_1, p_1)$, as follows:

Set $\sum_{k=2}^{K}\mathbf{H}_k\mathbf{S}_k\mathbf{H}_k^T + \mathbf{S}_z = \mathbf{Q}^T\mathbf{\Lambda}\mathbf{Q}$ be an eigenvalue decomposition, where $\mathbf{\Lambda}$ is a diagonal matrix and $\mathbf{Q}$ is an orthogonal matrix.

Let $\mathbf{\Lambda}^{-\frac{1}{2}}\mathbf{Q}\mathbf{H}_1 = \mathbf{U}\begin{bmatrix} c_{1,1} & & \\ & \ddots & \\ & & c_{1,\mathrm{n}} \end{bmatrix}\mathbf{V}^T$ be a singular value decomposition, where **U** and **V** are orthogonal matrices.

The optimal $\mathbf{S}_1 = \mathbf{V}\begin{bmatrix} \left(\frac{1}{2\lambda} - \frac{1}{c_{1,1}^2}\right)_+ & & \\ & \ddots & \\ & & \left(\frac{1}{2\lambda} - \frac{1}{c_{1,n}^2}\right)_+ \end{bmatrix}\mathbf{V}^T$.

The optimal $p_1 = \sum_{j=1}^{n}\left(\frac{1}{2\lambda} - \frac{1}{c_{1,j}^2}\right)_+$ where $(\cdot)_+ = min(0,\cdot)$.

The next step to repeat the same procedure for $(\mathbf{S}_2, p_2)$ while keeping other parameters $(\mathbf{S}_1, p_1) \ldots (\mathbf{S}_k, p_k)$ fixed.

(e) If $\sum_{k=1}^{K} p_k > P$, then set $l_{max} = l_{max} - (l_{max} - l_{min}) \times (0.5 - \gamma)$, otherwise set $l_{min} = l_{min} + (l_{max} - l_{min}) \times (0.5 - \gamma)$.

(f) If $|l_{min} - l_{max}| \leq 1$, stop. Otherwise go to step (b).

CHAPTER 4

4 Uplink Result and Analysis

4.1 Normalization

To better understand the relative performance improvement of the system using multi-sector cooperation, normalization of the channel is introduced in the analysis.

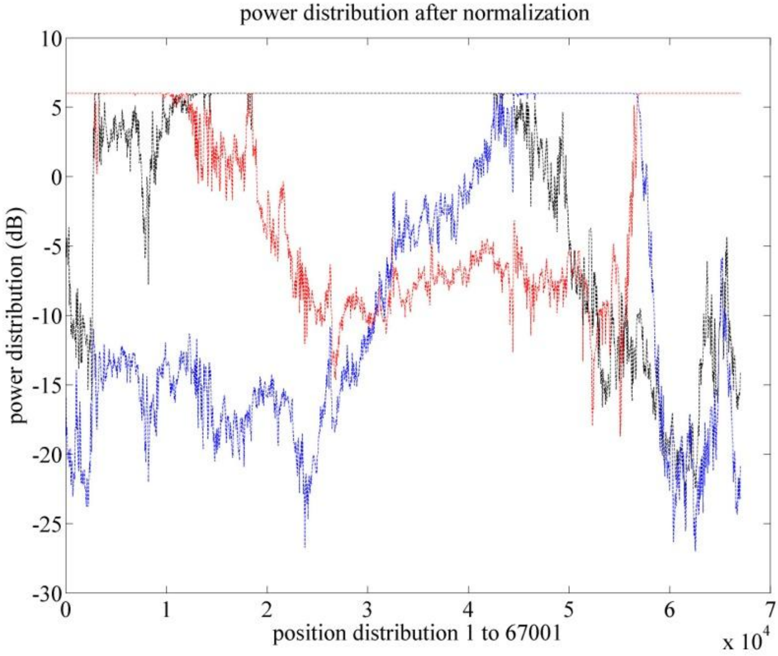

Fig. 4.1 Power distribution along the measurement locations. The red curve stands for the link of Sector 1, the black curve stands for the link of Sector 2, and the blue curve stands for the link of Sector 3.

The measured channels are normalized with respect to the single-sector link with the strongest power. The normalization is performed for all single-sector links, as well as the three-sector cooperative links. Figure 4.1 shows the power distributions of the links after the channel normalization for the 67001 measurement locations.

After the normalization, we get the same strongest channel power at each location. As can be seen in Fig. 4.1, the strongest single-sector link changes according to the location of the terminal along the drive route.

To better understand the power change of each sector and therefore find out the interface points (edges of two neighboring sectors), we translate the measurement locations to the angular locations with respect to the BS (see Fig. 4.2). We assume that the angular location starts (i.e., angle 0°) at the east position in Fig. 2.1 and increases along the counter-clockwise direction. Since the GPS data on the measurement locations have limited resolution, there can be more than one channel realization related to a given angular location in Fig. 4.2.

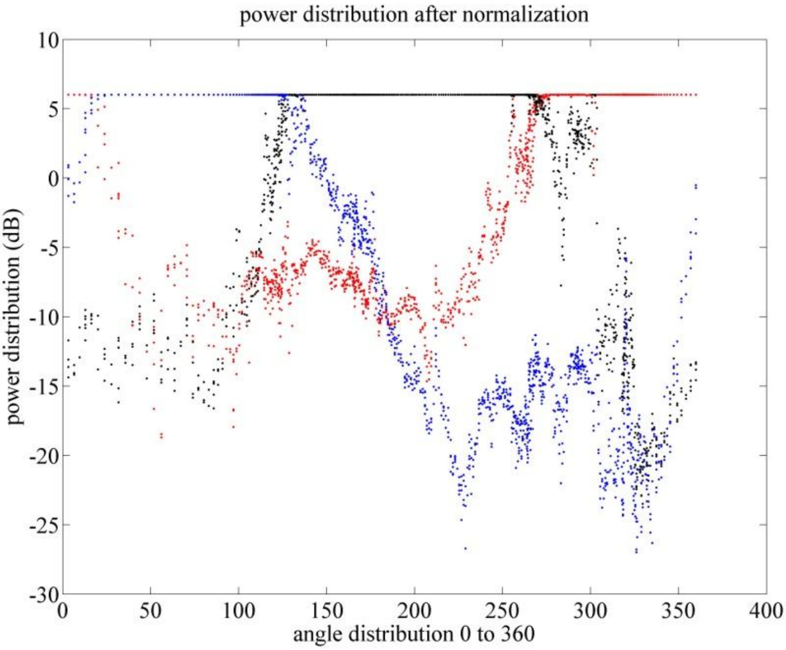

Fig. 4.2 Power distribution along the direction of the measurement locations. The red curve stands for the link of Sector 1, the black curve stands for the link of Sector 2, and the blue curve stands for the link of Sector 3.

Based on Fig. 4.2, it is clear that the angular directions 15°, 125° and 270° correspond to the sector edges. Even though the coverage of each sector was planned to be 120°, the power distribution based on the real data demonstrates that the actual coverage of each sector is not exactly 120°.

In order to better describe the sector distribution along the route locations, we draw the actual sector edges together with the drive route on the map, as in Fig. 4.3. Figure 4.3 will be referred to extensively in the following analysis.

It is obvious that Sector 2 has the largest coverage area of approximately 150°. On the other hand, the shortest distance between the route and the BS antennas is found in Sector 3. In addition, the start point and the end point are in Sector 1.

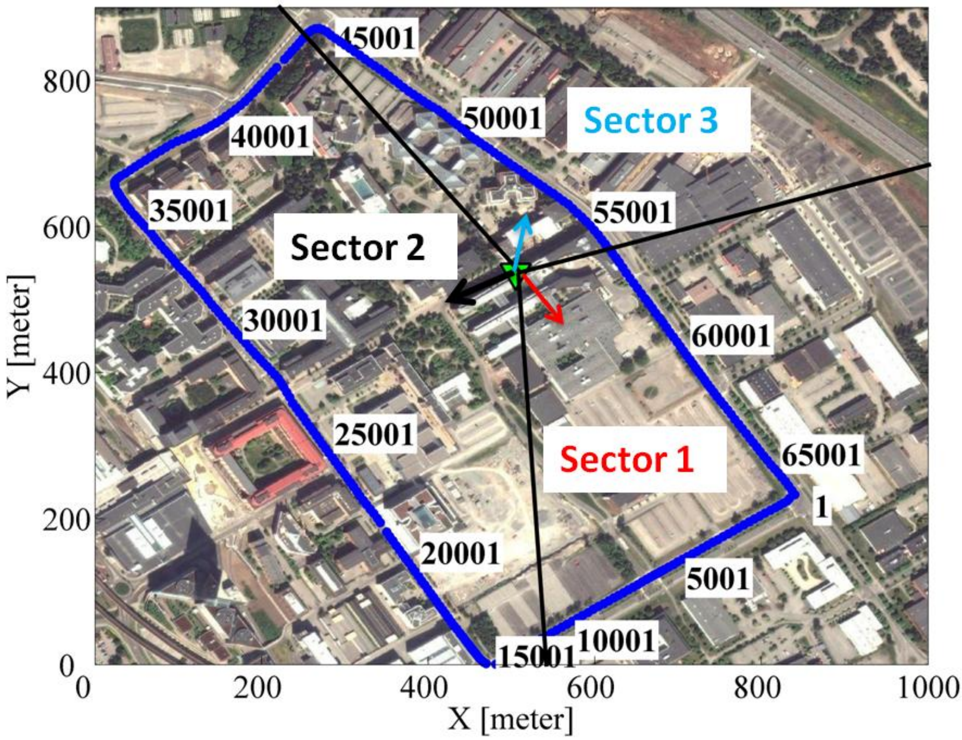

Fig. 4.3 Drive route with actual sector edges indicated.

4.2 Single-sector and cooperative uplink capacity analysis

According to the MIMO-MAC sum rate capacity formula (3-5), in order to calculate single sector uplink capacity for a scenario with a fixed user and a mobile user, we set reference $SNR = \frac{E_{s,1}}{N_0} = \frac{E_{s,2}}{N_0} = 10$, and $\mathbf{H}_1$ and $\mathbf{H}_2$ are the channels for the fixed user and the mobile user, respectively. In the non-cooperation case, at each mobile position, both $\mathbf{H}_1$ and $\mathbf{H}_2$ (2×2 matrices) have only one serving sector, which means only Sector 1 or Sector 2 or Sector 3 serves the two users around the drive route.

Figure 4.4 is a randomly chosen example of uplink capacity served by a single sector when the mobile user moves along each measurement location of the drive route, while the fixed user stays at the position 34000. The uplink capacity varies with the mobile user positions and the sector considered.

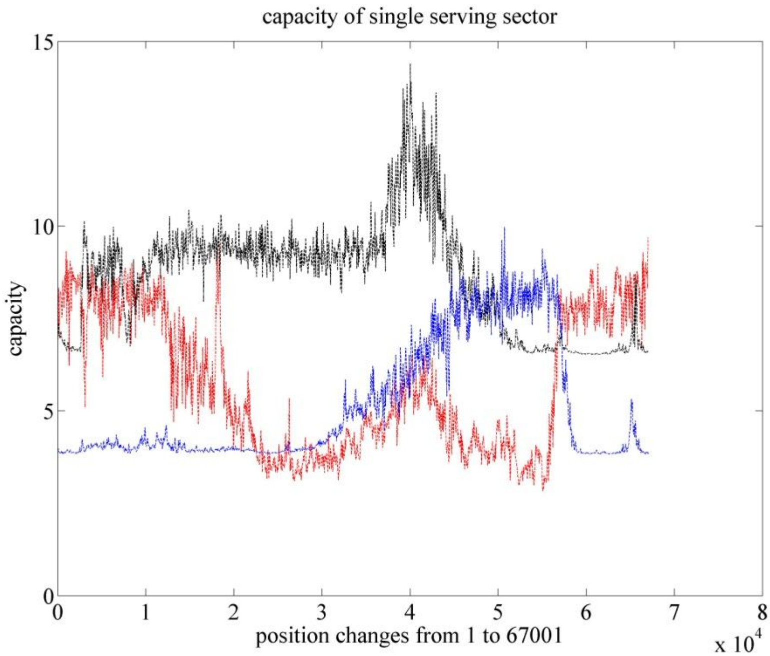

Fig. 4.4 Uplink capacity (bps/Hz) for single sector when fixed user at 34000. The red curve stands for the link of Sector 1, the black curve stands for the link of Sector 2, and the blue curve stands for the link of Sector 3.

It is clear that the single-link sum capacity of Sector 2 (black curve) is higher than that of Sector 1 (red curve) or Sector 3 (blue curve) at most locations. This is because the randomly chosen position 34000 for the fixed user is located in the coverage area of Sector 2. Therefore, when the mobile user moves within Sector 2, both the fixed and mobile users are in the coverage area of serving Sector 2. This can lead to strong channels for the two users, which result in high sum capacity values. As shown in Fig. 4.4, the capacity from positions 13350 to 44000 is higher than the capacity for other positions. In another word, when the serving sector is Sector 1 or Sector 3, there is at least one user outside the coverage area of the serving sector, which greatly decreases the channel strength and therefore decreases the capacity value.

On the other hand, it is observed that there are some positions where Sector 1 or Sector 3 provides higher capacity to the two users than Sector 2. At these positions, the two users are located in the coverage areas of two different sectors, with one user suffering from a weak channel. Therefore, it is possible for Sector 1 or Sector 3 to provide stronger channels for the two users in these positions, relative to Sector 2.

Similarly, the calculation of the three-sector cooperative uplink capacity uses the same formula and the same scenario of a fixed user and a mobile user. Again, we set $SNR = \frac{E_{s,1}}{N_0} = \frac{E_{s,2}}{N_0} = 10$. But $\mathbf{H}_1$ and $\mathbf{H}_2$ (now 6×2 matrices) are the user channels served by three sectors cooperatively. The capacity result is given in Fig. 4.5.

The shape of the capacity curve in Fig. 4.5 is different to the Sector 2 capacity in Fig. 4.4. In particular, the absolute value of the capacity is higher for the three-sector cooperation case. The percentage capacity increase due to sector cooperation is shown in Fig. 4.6. From Fig. 4.6, we can conclude that cooperation significantly increases the capacity, which is almost doubled in value for some positions. Moreover, the average capacity increase is 35%, which further confirms the effectiveness of cooperation in providing capacity gain.

However, in order to better understand the characteristics of capacity gain due to cooperation, in the following, we choose the location of the fixed user based on the power distribution Fig. 4.2.

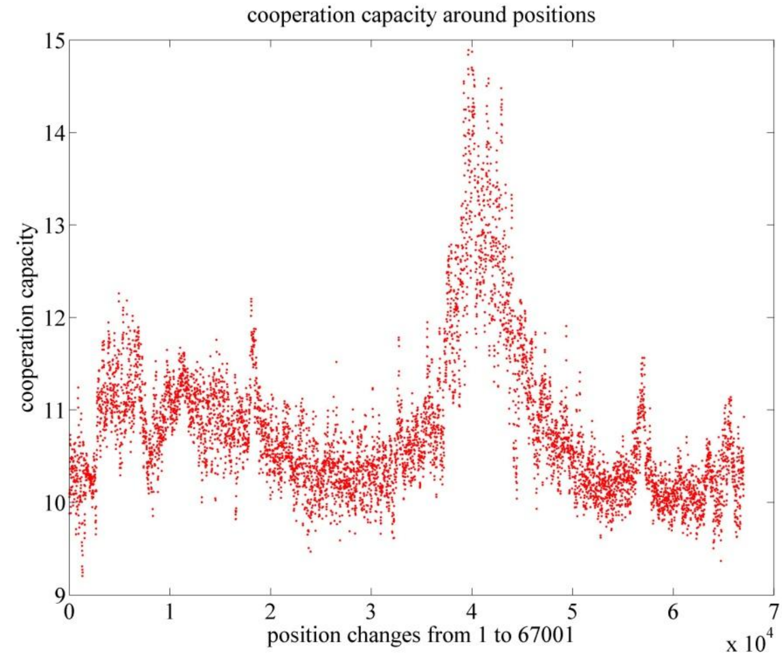

Fig. 4.5 Uplink cooperative capacity (bps/Hz) when the fixed user is at position 34000.

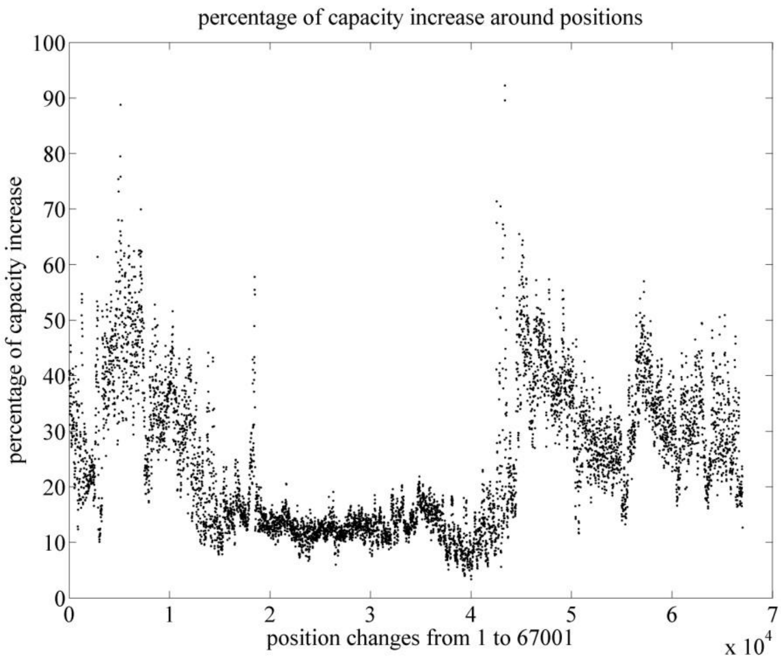

Fig. 4.6 Uplink percentage capacity gain when the fixed user is at position 34000.

On the one hand, we will check the percentage increase in capacity when the fixed user stays at the location with the strongest channel of each sector, which means the center of each sector. Based on Fig. 4.3, the index of the center location for each of the three sectors is shown in Table 4.1. With this information, we will study the how the percentage capacity increase with cooperation varies with the mobile user location when we set the fixed user at the sector center locations. On the other hand, we will also investigate whether the trend of the percentage capacity increase will be the same if the fixed user is moved to the edge of the serving sector.

TABLE 4.1 INDEX OF POSITION AT THE CENTER OF EACH SECTOR

Specification	Index of Position
Center of Sector 1	2442
Center of Sector 2	27627
Center of Sector 3	50514

The choice of these two study cases is based on the fixed user being placed at two extremities of the serving sector (i.e., sector center or sector edge), in terms of the channel gain. Moreover, it will be too complicated to consider all possible positions of the two users in the analysis.

From Figs. 4.7 to 4.9, it is concluded that when the fixed user is at the center of the serving sector, the sum capacity will be increased the most when the mobile user moves to the back lobe region of the fixed user's serving sector. The percentage of capacity gain can be up to 178%. In this condition, cooperation plays an important role for the mobile user by increasing the received channel power.

However, upon studying the cumulative distribution functions (CDFs) in Figs. 4.7 to 4.9, it is observed that the median capacity gain is only around 30%. The reason is that cooperation can greatly improve the capacity only when the serving sector does not provide adequate power to one of the two users.

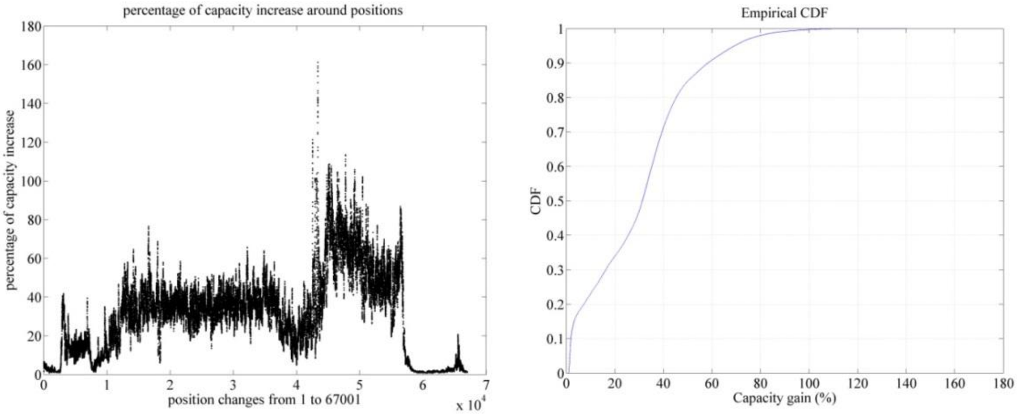

Fig. 4.7 Uplink capacity gain and CDF when the fixed user is at position 2442.

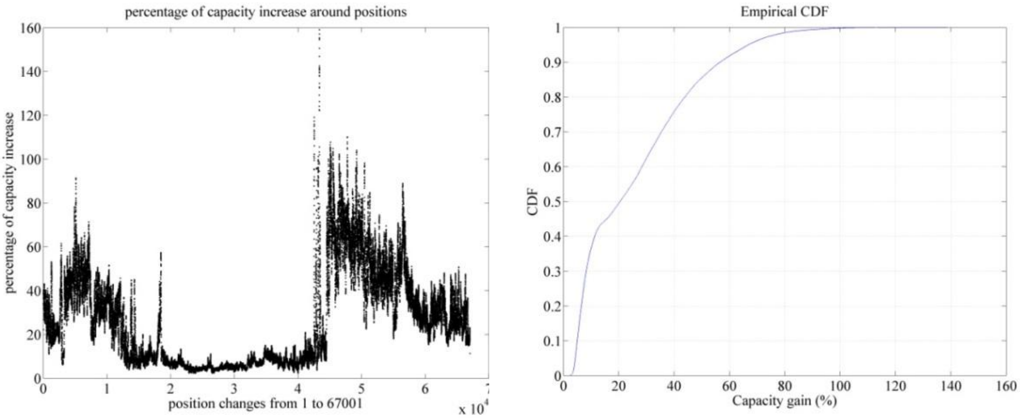

Fig. 4.8 Uplink capacity gain and CDF when the fixed user is at position 27627.

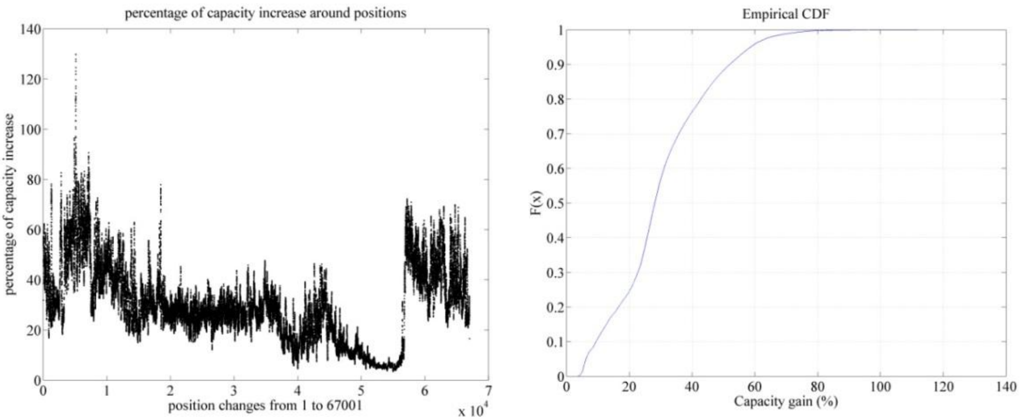

Fig. 4.9 Uplink capacity gain and CDF when the fixed user is at position 50514.

Moreover, there is about 33% probability that the two users are located in the same sector (for the given drive route shown in Fig. 4.3), which is when capacity can hardly be increased through cooperation with two other sectors. Nevertheless, 10% of the positions have capacity gains of over 60% according to the CDFs, showing that cooperation can significantly improve the capacity for some user locations.

Next, we will check the condition when the fixed user is located at the edges of two neighboring sectors, i.e., where two sectors provide almost equal channel power and the influence of the third sector is negligible. The indices of these positions are given in Table 4.2. Figures 4.10-4.12 show the percentage capacity gain in this study case.

TABLE 4.2 INDEX OF SECTOR EDGE OF NEIGHBORING SECTORS

Specification	Index of Positions
Edge of Sector 1 and Sector 2	9859
Edge of Sector 2 and Sector 3	44920
Edge of Sector 1 and Sector 3	56787

Comparing Fig. 4.10 with the map in Fig 4.3, it is obvious that when the fixed user is located at the edge of Sector 1 and Sector 2 and the mobile user moves into Sector 3, the capacity improvement is maximized. Moreover, 10% of the mobile user positions provide capacity gains of over 80%.

The reason for the observed maximized capacity gain is that without the sector cooperation, when two users are served by one sector, these locations of fixed user and mobile user are where the serving sector offers the weakest channels for both users, which lead to the weak sum rate capacity. To be more specific, without cooperation, when the fixed user is located at the edge of Sector 1 and Sector 2 and the mobile user is located at Sector 3, no matter which sector is the serving sector, the fixed user will still suffer from a weak channel.

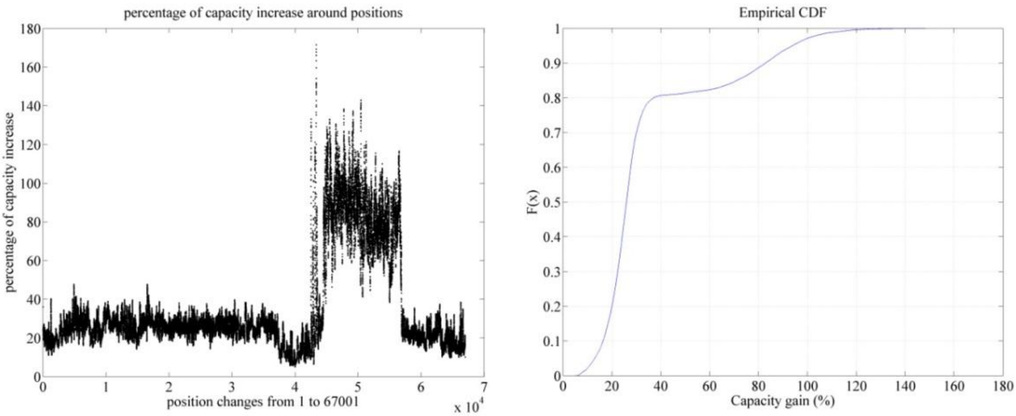

Fig. 4.10 Uplink capacity gain and CDF when the fixed user is at position 9859.

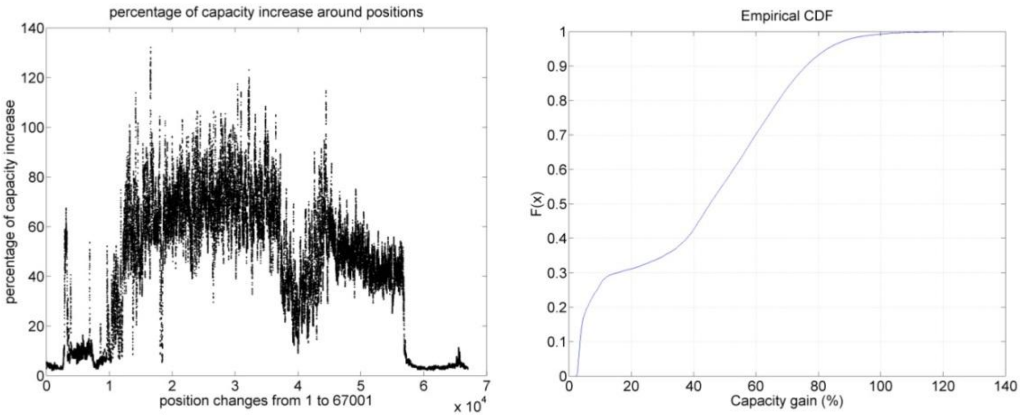

Fig. 4.11 Uplink capacity gain and CDF when the fixed user is at position 56787.

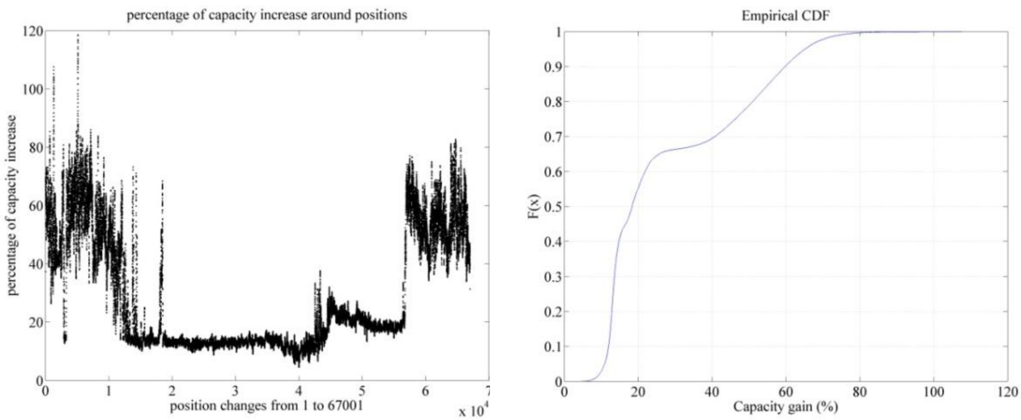

Fig. 4.12 Uplink capacity gain and CDF when the fixed user is at position 44920.

To further prove the above speculation, we study Figs. 4.11 and 4.12, which correspond to the fixed user being located at the other two sector edges, respectively. Fig. 4.11 is the situation when the fixed user is located at the edge of Sector 1 and Sector 3 (position 56787), while Fig. 4.12 is the situation when the fixed user is located at the edge of Sector 2 and Sector 3 (position 44920).

As can be seen in Fig. 4.11, when the fixed user is locates at the edge of Sector 1 and Sector 3, the capacity is increased dramatically (i.e., about 100%) when the mobile user moves into Sector 2. In addition, the median capacity gain is almost 50%. Similarly, when the fixed user is located at the edge of Sector 2 and Sector 3, the capacity shows greatly improvement when the mobile user moves into Sector 1.

Therefore, we can conclude that when one user is fixed at the edge of two sectors, the capacity gain due to cooperation is increased dramatically when the other user moves into the third sector.

CHAPTER 5

5 Downlink Result and Analysis

As introduced in Chapter 3, duality algorithm and formula (3-8) are used in the calculation of downlink capacity. Normalizations of the channels are the same as we have done in Chapter 4.

Firstly, we will still study the randomly chosen example of Chapter 4, i.e., when the fixed user is located at the position 34000 (within Sector 2), while the mobile user moves around the drive route. Figures 5.1(a) to 5.1(c) show the downlink sum capacity when the serving sector is Sector 1, Sector 2 and Sector 3, respectively. As can be seen, high capacity values are obtained when the mobile user moves to the coverage area of the serving sector. Moreover, the maximum capacity values (i.e., between 8.2 to 8.4 bps/Hz) are achieved when both users are located in the serving sector, as can be observed in Fig. 5.1(b).

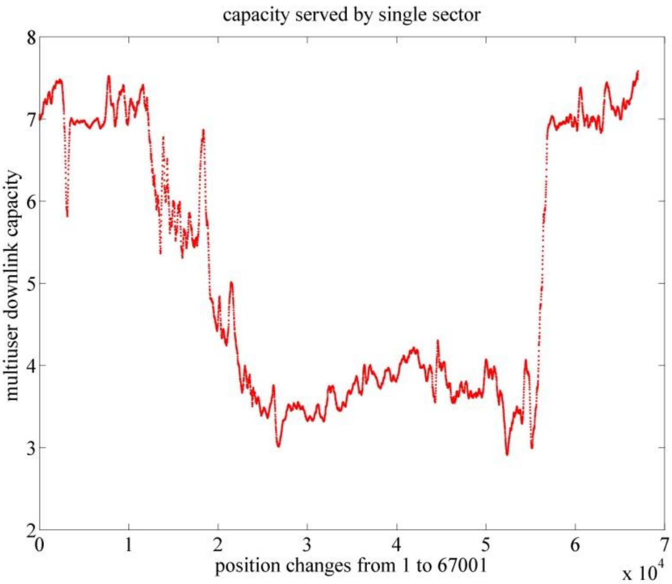

(a) Downlink capacity (bps/Hz) served by Sector 1.

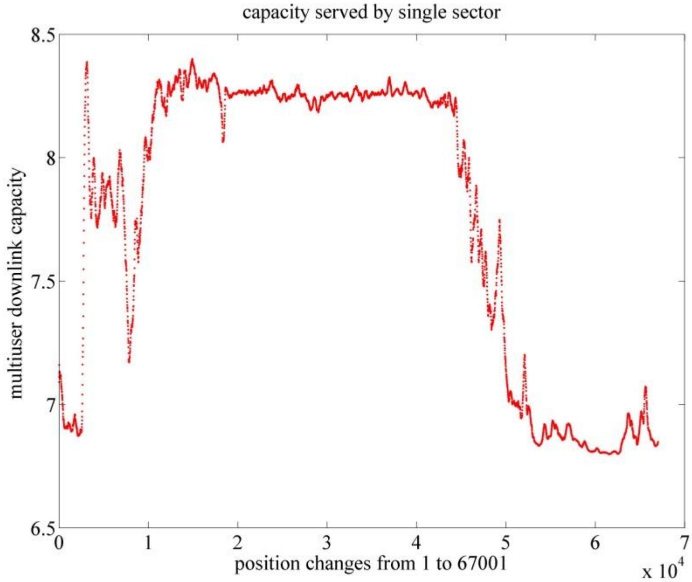

(b) Downlink capacity (bps/Hz) served by Sector 2.

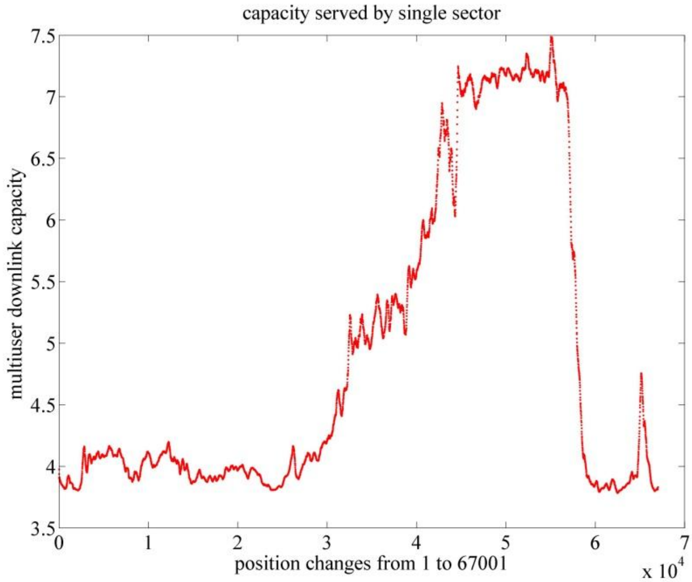

(c) Downlink capacity (bps/Hz) served by Sector 3.

Fig. 5.1 Downlink sum capacity of each single serving sector when the fixed user is at position 34000.

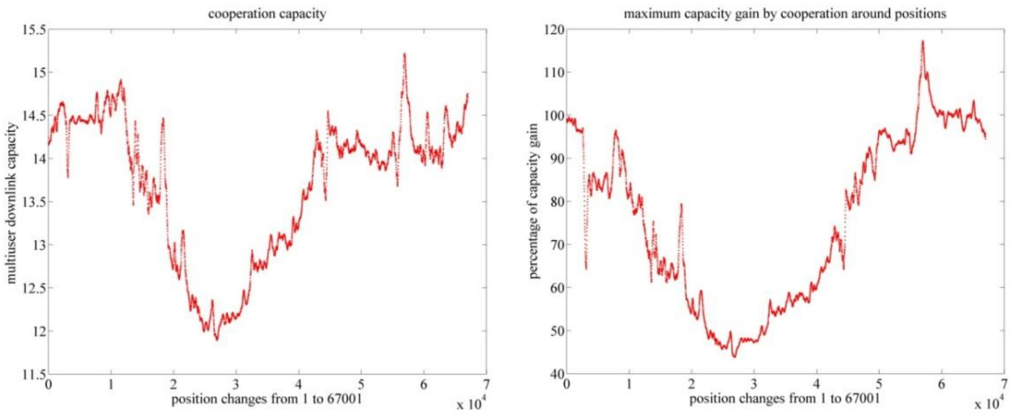

Fig. 5.2 Downlink capacity (bps/Hz) with sector cooperation when the fixed user is at position 34000 (left); Percentage of capacity gain relative to the best single sector capacity at each position (right).

According to Fig. 5.2, the downlink capacity has been greatly improved through sector cooperation, and the lowest capacity value after cooperation is still higher than the highest single-sector capacity value. The percentage of capacity gain shown in the right plot of Fig. 5.2 is obtained by comparing the capacity with cooperation against the highest single serving sector capacity at each position. The lowest gain is 50%, which shows the effectiveness of sector cooperation in the downlink case.

But since the above example is a random one, in order to demonstrate the capacity gain through cooperation more comprehensively, we choose the location of the fixed user to be at the center of a given sector or the edge of neighboring sectors, as had been done for the uplink case in Chapter 4.

The position index of each sector's center is the same as those shown in Table 4.1. The results for the fixed user located at sector centers are presented in Figs. 5.3 to 5.5: single sector capacity, cooperation capacity, capacity gain through cooperation and CDF behavior.

According to Figs. 5.3 to 5.5, the median capacity gain is over 70% and 10% of the positions have at least doubled in capacity. Furthermore, it is noted that when the fixed user is located at the center of a given serving sector, the capacity greatly increases when the mobile user moves to the back lobe region of the serving sector. The reason for this phenomenon is explained as follows. If the two users are located in two different sectors (one being the serving sector), without cooperation, only one user will experience a strong channel (i.e., the one in the serving sector) while the other user will suffer from weak channel from the serving sector. In this case, cooperation can greatly enhance the weak channel and increase the system capacity. This is especially the case when the mobile user moves to the back lobe of the serving sector, since the mobile user experiences the weakest possible channel from the serving sector in this case.

Then, we also examine the condition when the fixed user stays at the edge of the neighboring sectors. The relevant position indices have been presented earlier in Table 4.2, for the uplink study. Figs. 5.6 to 5.8 give the results for the three cases of the fixed user located at a sector edge: single sector capacity, cooperation capacity, capacity gain through cooperation and CDF behavior.

Based on Figs. 5.6 to 5.8, it can be noted that the capacity can be increased by more than 60% at the minimum, and at least 10% of the positions can get an increase of over 100%. This provides the evidence that sector cooperation is particularly effective when one user is kept at the edge of two sectors. Moreover, according to the capacity gain figures, we can conclude that when the mobile user moves to the main lobe direction of the third sector (i.e., with the fixed user located at the edge of the two other sectors), the downlink capacity improvement is maximized. This is because the fixed user is at the position with the weakest channel (sector edge) and likewise the mobile user is located outside the serving sector. Therefore, the cooperation significantly increases the power received at the fixed user due to the power from the neighboring sector, and at the same time it enables the mobile user to receive the maximum available power from the third sector.

It is also observed that in this case, the biggest cooperation capacity value does not appear at the same position as where the system has the greatest capacity gain. This is because certain positions have strong channels by themselves (without cooperation). Even though the cooperation does not contribute much to the strength of the channel, these positions can still have better capacity performance. After checking the map in Fig. 4.3 carefully, it is found that these positions correspond to LOS scenarios.

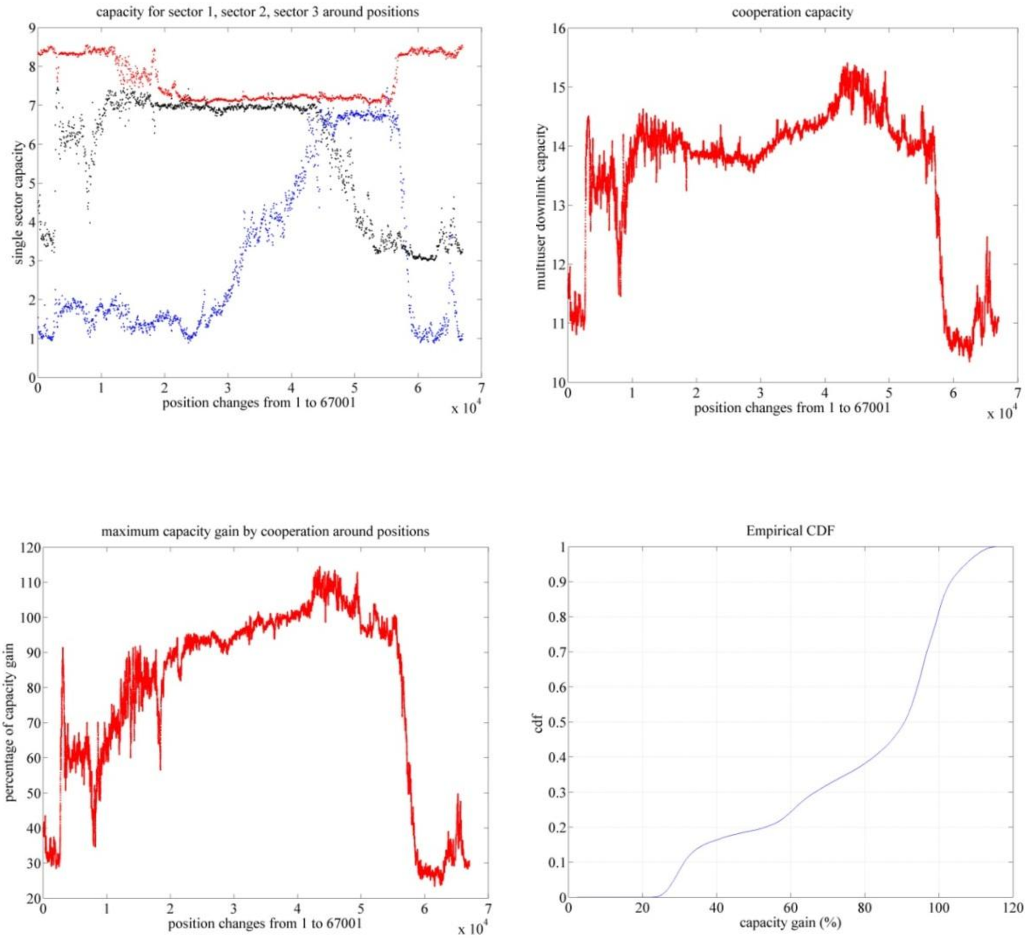

Fig. 5.3 Fixed user located at position 2442. For the upper left plot, the red curve stands for the link of Sector 1, the black curve stands for the link of Sector 2, and the blue curve stands for the link of Sector 3. Similar color coding is used in Figs. 5.4 to 5.8.

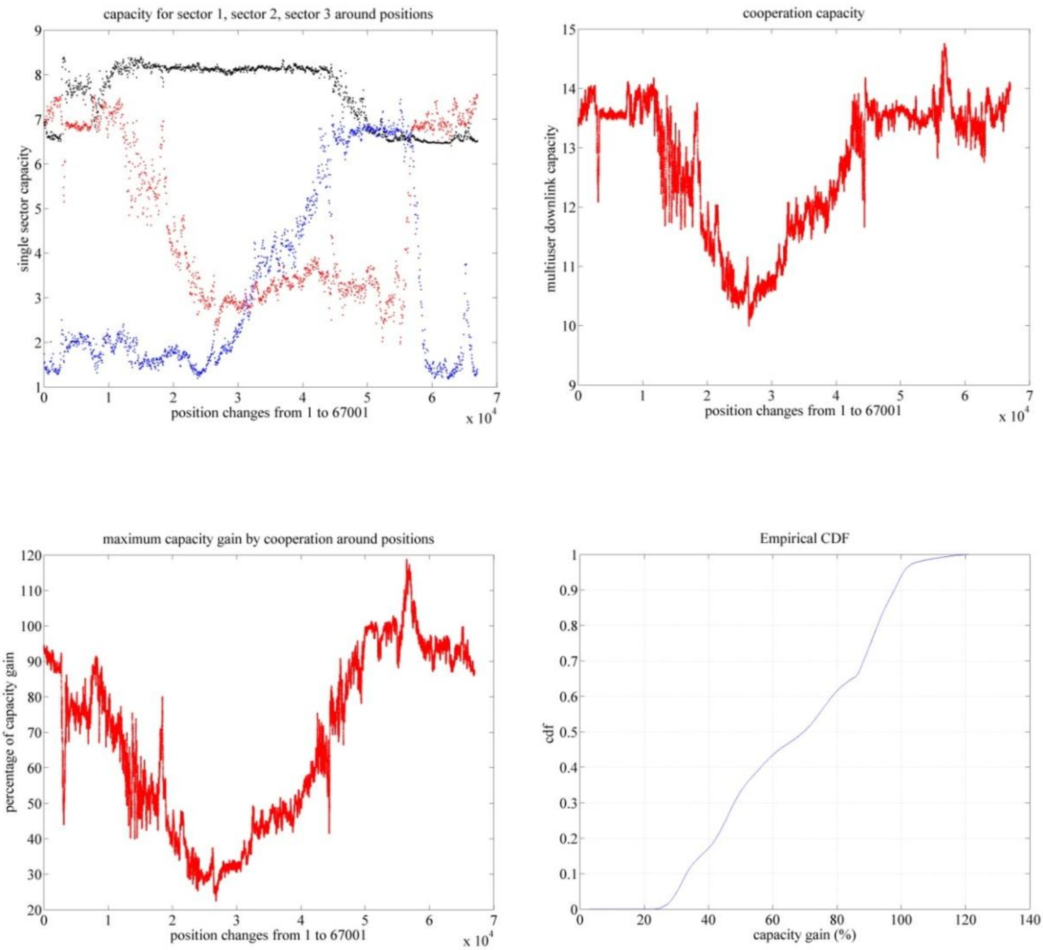

Fig. 5.4 Fixed user located at position 27627.

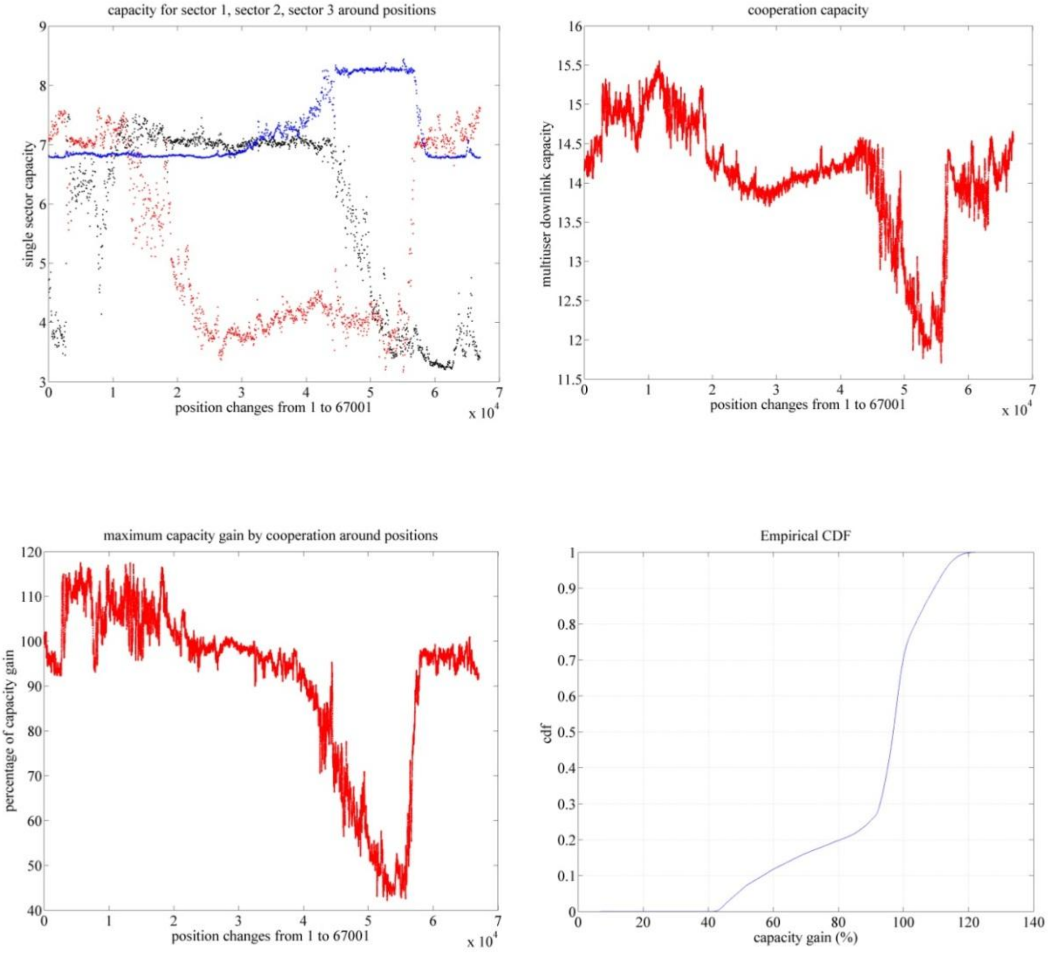

Fig. 5.5 Fixed user located at position 50514.

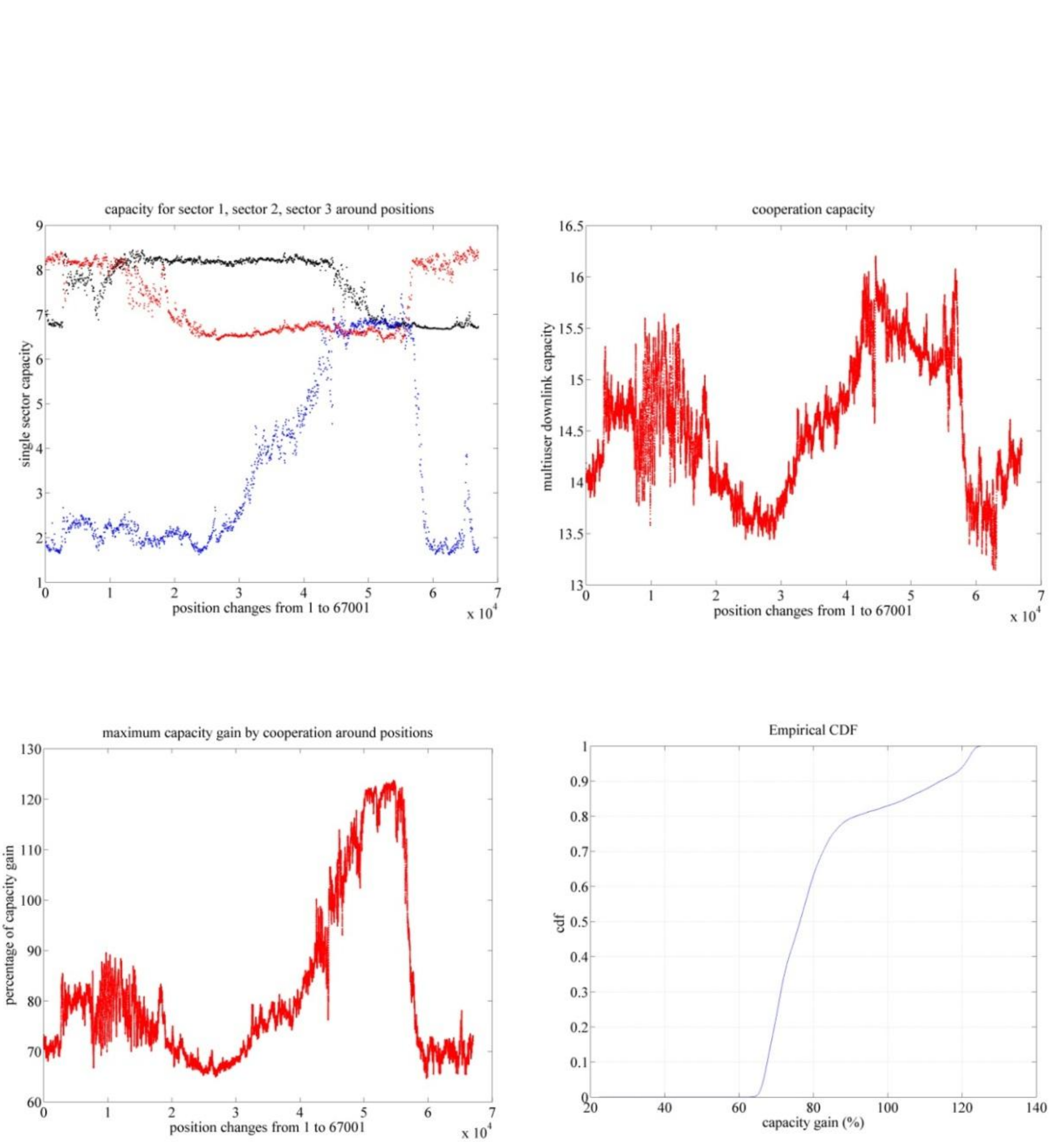

Fig. 5.6 Fixed user located at position 9859.

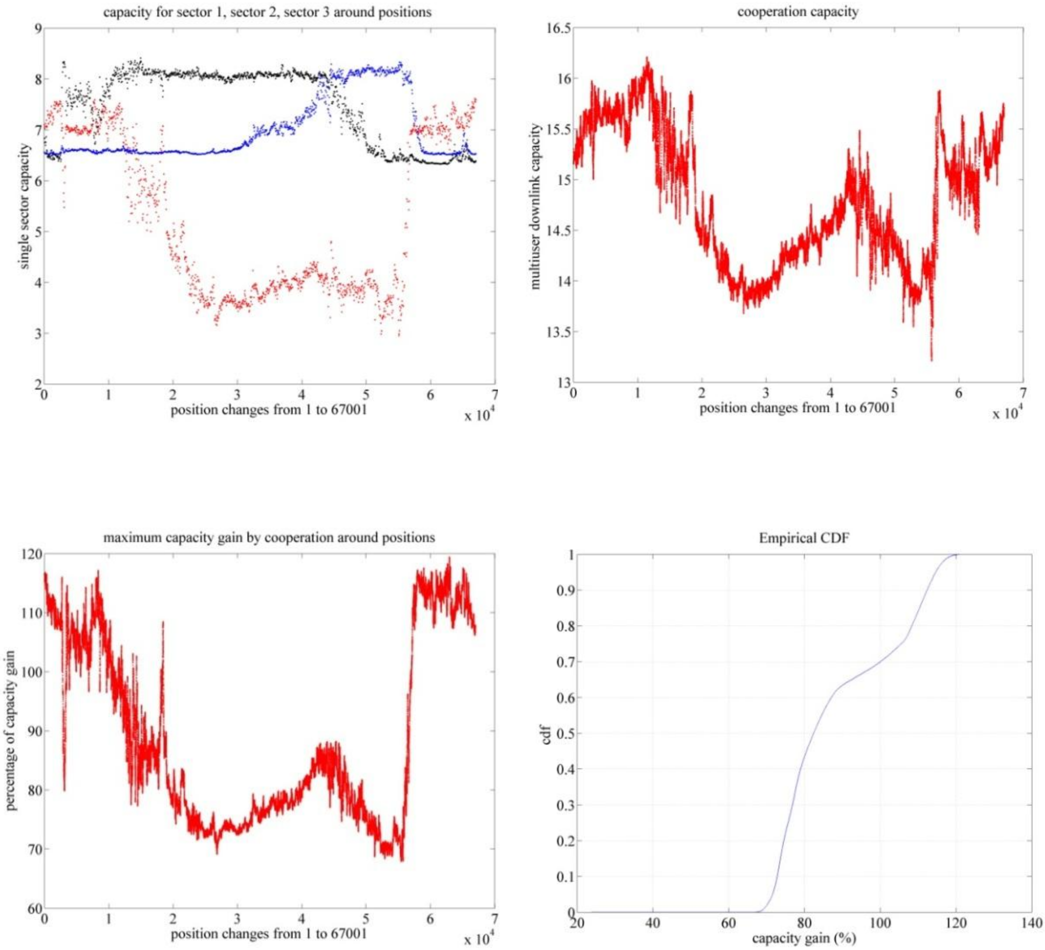

Fig. 5.7 Fixed user located at position 44920.

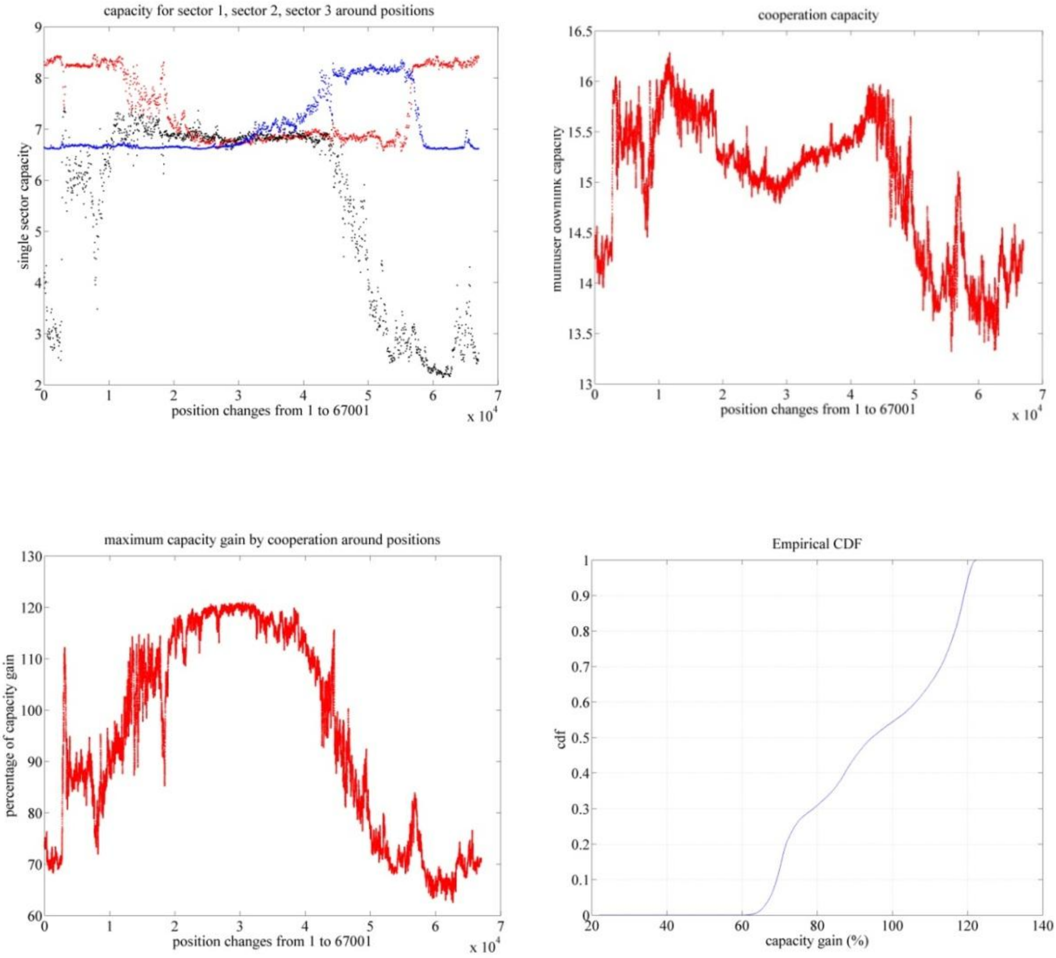

Fig. 5.8 Fixed user located at position 56787.

CHAPTER 6

6 Conclusion

6.1 Capacity gain

We will first look at the capacity gain of the uplink case based on the results we obtained in Chapter 4. According to the CDFs, we find that the median capacity gain is 30% and about 10% of the positions achieve capacity gains of more than 80%.

On the other hand, sectors cooperation is more effective in the downlink case according to the results we obtained in Chapter 5. It is clear that the median capacity gain is 65% and around 10% of the positions get capacity gains of more than 110%.

Moreover, no matter in which situation, sector cooperation has proved its advantage in increasing the system capacity.

As for the relatively better performance in the downlink case, it is noted that even though the duality method can convert the downlink model into an uplink model, the formulas used in the calculation of the uplink and downlink capacity are different.

To be more specific, for time-varying MIMO channels, there are multiple capacity definitions and models. In our case, we choose the joint decoding method in the MAC capacity calculation. However, the capacity formula for BC after the duality conversion is not the same. Therefore, it is reasonable to get different results.

6.2 Comparison between downlink and uplink

We came to similar conclusions for both the downlink and uplink cases when we studied the following two scenarios: fixed user located at the center of each sector and the fixed user located at the edge of two neighboring sectors.

When one user is located at the center of a given sector, and the other user moves to the back lobe of this sector, the system will get the maximum capacity gain with sector cooperation.

When one user is located at the edge of two neighbor two sectors, the other user moves in the region of the third sector, the system capacity can be greatly improved through sectors cooperation.

CHAPTER 7

7 Future Work

After the careful investigation on the MU-MIMO capacity performance, we have successfully demonstrated the value of sector cooperation at the BS side. However, other scenarios can be studied as future work.

For example, the reference case in this work is based on one serving sector, even when not all users are located within the serving sector. A more realistic case is to consider the reference scenario where each user is served by its own serving sector, which is not necessarily the same for multiple users. It will be interesting to study how this new reference case will influence the results on capacity gain from cooperation.

In addition, we have mainly considered two cases: fixed user located at the center and fixed user located at the edge of two neighboring sectors. It is possible that some other ways of placing the users may yield interesting conclusions.

Furthermore, we focused on the joint decoding method in MAC and the duality algorithm in BC for the capacity calculation. Other schemes can also be examined.

References

[1] T. Nakamura, “LTE and LTE-Advanced: Radio technology aspects for mobile communications ,” in *Proceedings of the XXX-th General Assembly and Scientific Symposium*, Turkey, Istanbul, Aug 13-20, 2011, pp. 1-4.

[2] A. F. Molisch, *Wireless Communications*, 2nd Ed, Wiley, 2011.

[3] J. Zhang, G. Liu, F. Zhang, L. Tian, N. Sheng, and P. Zhang, “Advanced international communications,” *IEEE Veh. Technol. Mag.*, vol. 6, no. 2, pp. 92-100, Jun. 2011

[4] A. Paulraj, R. Nabar and D. Gore, *Introduction to Space-Time Wireless Communications*, Cambridge University Press, 2003.

[5] D. Gesbert, M. Kountouris, R. W. Health, C. B. Chae, and T. Zaler, “Shifting the MIMO paradigm,” *IEEE Signal Process. Mag.*, vol. 24, no. 5, pp. 36 - 46, Sep. 2007.

[6] G. Bauch and A. Alexiou, “MIMO technologies for the wireless future,” in *Proceedings of the IEEE PIMRC 2008*, Cannes, France, Sep. 15-18, 2008, pp. 1-6.

[7] F. Kaltenberger, M. Kountouris, D. Gesbert, and R. Knopp, “On the trade-off between feedback and capacity in measured MU-MIMO channels ,” *IEEE Trans. Wireless Commun.*, vol. 8, no. 9, pp. 4866-4875, Sep. 2009.

[8] B. Mondal, T. A. Thomas, and A. Ghosh, “MU-MIMO system performance analysis in LTE evolution,” in *Proceedings of the IEEE PIMRC 2010*, Istanbul, Turkey, Sep. 26-29, 2010, pp. 1510-1515.

[9] D. Lu, H. Yang, K. Wu, “On the feedback enhancement and system performance evaluation of downlink MU-MIMO for 3GPP LTE-Advanced,” in *Proceedings of the IEEE 73rd Vehicular Technology Conference*, Budapest, Hungary May 15-18, 2011, pp. 1-5.

[10] J. Duplicy, B. Badic, R. Balraj, and R.Ghaffar, “MU-MIMO in LTE systems,” *EURASIP Journal on Wireless Communications and Networking*, vol.2011, no., pp 1-14, ISSN, February 2011

[11] F. Liang, M. Yang, P. Gong, and W. Wu, “A joint TX-RX user scheduling scheme for multiuser MIMO systems,” in *Proceedings of the 5th International Conference on Wireless Communications, Networking and Mobile Computing (WiCOM)*, Beijing, China , Sep. 24-26, 2009, pp. 1-5.

[12] Y. Nam, L. Liu, Y. Wang, C. Zhang, J. Cho, and J. Han, “Cooperative communication technology for LTE-Advanced,” in *Proceedings of the IEEE International Conference on Acoustics Speech and Signal Processing (ICASSP)*, pp. 5610-5613, Dallas, USA, Mar. 14-19, 2010.

[13] R. Irmer, H. Droste, P. Marsch, M. Grieger, G. Fettweis, S. Brueck, H. Thiele, and V. Jungnickel, “Coordinated multipoint: Concepts, performance, and field trial results,” *IEEE Commun. Mag.*, vol. 49, no. 2, pp. 102-111, Feb. 2011.

[14] V. Jungnickel, S. Jaeckel, L. Thiele, L. Jiang, U. Krüger, A. Brylka, and C. Helmolt, “Capacity measurements in a cooperative MIMO network,” *IEEE Trans. Veh. Technol.*, vol. 58, No. 5, pp. 2392-2405, Jun. 2009

[15] L. Thiele, T. Wirth, M. Schellmann, Y. Hadisusanto, and V. Jungnickel, “MU-MIMO with localized downlink base station cooperation and downtilted antennas,” in *Proceedings of the IEEE International Conference on Communication Workshops*, Dresden, Germany, Jun. 14-18, 2009, pp. 1-5.

[16] S. Han, Q. Zhang, and C. Yang, “Distributed coordinated multi-point downlink transmission with over-the-air communication,” in *Proceedings of the 5th International ICST Conference on Communications and Networking in China (CHINACOM)*, Beijing, China , Aug. 25-27, 2011, pp. 1-5.

[17] B. Suard, G. Xu, and T. Kailath. “Uplink channel capacity of space-division-multiple-access schemes,” *IEEE Trans. Inform. Theory*, vol. 29, no. 3, pp. 439-441, Jul. 1998.

[18] M. Costa, “Writing on dirty paper,” *IEEE Trans. Inform. Theory*, vol. 44, no. 4, pp. 1468-1476, May 1983.

[19] W. Yu, “Uplink-downlink duality via minimax duality,” *IEEE Trans. Inform. Theory*, vol. 52, no. 2, pp. 361 - 374, Feb. 2006.

[20] S. Vishwanath, N. Jindal, and A. Goldsmith, “Uplink duality, achievable rates, and sum-rate capacity of Gaussian MIMO broadcast channels,” *IEEE Trans. Inform. Theory*, vol. 49, no. 10, pp. 2658-2668, Oct. 2003.

[21] W. Yu, “Sum-capacity computation for the Gaussian vector broadcast channel via dual decomposition ,” *IEEE Trans. Inform. Theory*, vol. 52, no. 2, pp. 754-759, Feb. 2006.

List of Acronyms

BC	Broadcast Channel
CA	Carrier Aggregation
CDF	Cumulative Distribution Function
CDMA	Code Division Multiple Access
CoMP	Coordinated Multi-Point
CSI	Channel State Information
LOS	Light-of-Sight
LTE	Long Term Evolution
MAC	Multiple Access Channel
MIMO	Multiple-Input Multiple-Output
OFDMA	Orthogonal Frequency Division Multiple Access
QoS	Quality of Service
RX	Receive
SC-FDMA	Single-Carrier Frequency Division Multiple Access
SINR	Signal-to-Interference-and-Noise Ratio
SNR	Signal-to-Noise Ratio
TX	Transmit
UMTS	Universal Mobile Telecommunication System